EXPERIMENTAL DEMONSTRATION OF METAMATERIAL-BASED PHASE MODULATION

I. O. Mirza, J. N. Sabas, S. Shi, and D. W. Prather

Department of Electrical and Computer Engineering
University of Delaware
151 Evans Hall Newark, Delaware 19716, USA

Abstract—Phase modulation is critical due to its applicability in varied RF devices such as phased array antennas, radars to name a few. In this paper, we report experimental data on phase modulation in the X-band frequency using tunable metamaterials such as a planar design of stacked dual split ring resonators (DSRRs) of 3 mm thickness at 8.5 GHz. Modulation was brought about by switching between the open and closed states of the rings causing a net change in the effective refractive index and thereby producing a phase variation. One and two dimensional free-space scanning experiments were carried out where a phase modulation of 62 degrees was demonstrated. The measured data matched well with the numerically simulated results.

1. INTRODUCTION

Recently in the electromagnetic community, metamaterials have been instrumental in devising novel applications based on their atypical electromagnetic behavior [1–3]. Flat lenses based on negative refraction, miniaturized antennas using artificial inductive materials, beam scanning with forward-backward waves and more recently cloaking devices are a few of the groundbreaking applications with metamaterials [3, 16–18, 20, 27]. Furthermore, a resonating metamaterials' response can be further enhanced by effectively changing the material properties by introducing tunability within the structure. Along that line, it was shown that by varying the geometry of the inclusions or the refractive index of the metamaterial's host material, using electronic controls, tunability can be achieved

---

Corresponding author: I. O. Mirza (iomirza@udel.edu).

in terms of frequency shifting and amplitude modulation [4, 7–13, 15, 23]. Recently, Terahertz phase modulation was reported where the metamaterial was grown on GaAs and was modulated electrically [28]. A tunable phase modulator is also attractive in the RF/microwave frequency domain as it can have applications in phased array antennas and radars for beam-forming and beam scanning and can potentially set the platform for a spatial light modulator in this frequency regime [22, 25]. Previously, in the X-band frequency range, numerical results on metamaterial-based phase modulation were reported where two designs were considered based on the excitement of the input source. It was demonstrated that a net change in the phase angle of up to 80 degrees could be achieved in the X-band using a planar design of dual split ring resonators (DSRRs) [29]. The attractive features of this particular design were that the configured structure was relatively thin in the propagation direction of the incident wave and had low transmission loss due to its operation at an off-resonant frequency. In this paper we present a follow up on the previous report by experimentally demonstrating the modulation of phase using DSRRs fabricated on FR4 substrate and tuning it between the open and closed state of the rings. The structure consists of split ring resonators stacked together with adjacent rings oriented opposite to each other. Firstly, we performed numerical simulation for the proposed design where we noted the phase variation that occurred due to switching between the open and closed state of the rings. Following that, free-space measurement setups were built for measuring the amplitude and phase variation of the fabricated device. Particularly, we setup a one dimensional (1-D) and a two dimensional (2-D) measurement system and compared their results to ensure consistency of our measured data. We noted from both of our measurements the average phase variation was around 66 degrees while the average amplitude variation was about 1.6 dB. In the following sections we briefly present the numerical results, discuss our test setup and measured data along with the future directions of this research work.

2. NUMERICAL RESULTS

In this section we overview the numerical setup for calculating the phase modulation using the DSRRs. The setup is shown in Fig. 1(a), where two layers of DSRRs were printed on the FR4 substrate ($\varepsilon = 4.4$) and was excited by the electric field which was parallel to the gap of the rings with the k-vector perpendicular to the structure [6, 19, 21, 29]. For our numerical simulation we used Ansoft's HFSS commercial
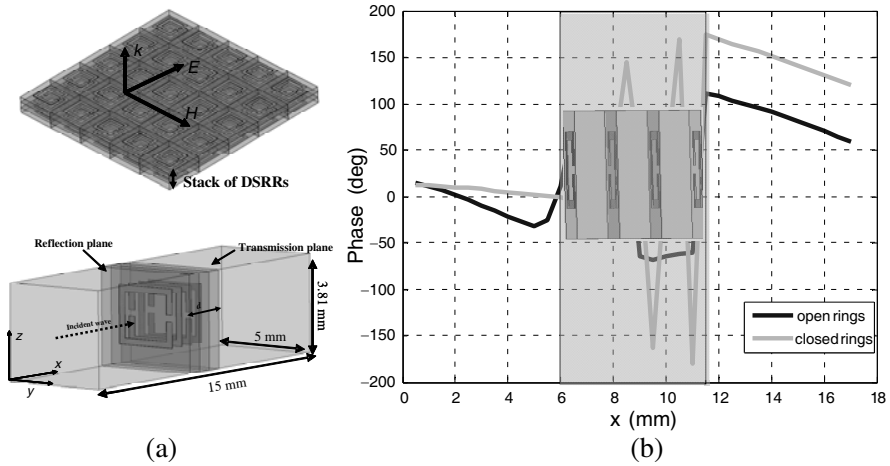
Figure 1. (a) Configuration for the planar DSRR slab. k-vector perpendicular to the slab. (b) Plot of the electric field line across the computational region indicating the phase information. Shaded region indicates the region occupied by the structure.

software. The total thickness of the stack was only 3 mm. The simulated structure was put in a computational region with dimensions of 15 mm×5 mm×3.81 mm with perfect electric conductor (PEC) and perfect magnetic conductor (PMC) boundary conditions in the z-direction and y-directions respectively. The reflection and transmission parameters extracted from the simulation were employed to locate and calculate the effective index of the slab at an off-resonance frequency [4, 5, 29]. In particular, the resonance of the stacked DSRRs occurred at a frequency of 9.15 GHz which provided an effective index of 4.9 for the open state and 3.3 for the closed state at an off-resonant frequency of 8.69 GHz (graphs not shown here). The large refractive index value of the closed ring case is due to the fact that a fraction of the substrate is occupied by metal portions- the closed rings. As such, the closed rings on the FR4 substrate exhibit a higher effective permittivity value than the FR4 substrate alone. The index contrast between the two states of the rings produced a phase variation according to $\Delta\phi = (\Delta n_{eff})kd$, where Δn_{eff} was the effective refractive index difference, d was the overall thickness of the stacked DSRRs, $k = \frac{2\pi}{\lambda}$, and $\Delta\phi$ is the phase difference. Thus, for this configuration, $\Delta n_{eff} = 4.9 - 3.3 = 1.6$, $d = \frac{3}{34.5}\lambda$. Therefore $\Delta\phi \sim 1.6 \times 2\pi/\lambda \times 0.1\lambda \simeq 50°$. We also verified this data by using the volumetric electric field information inside the computational region. This method was effective in the

sense that it would account for any multiple reflections that might occur within the slab and would provide the phase information in the free-space after exiting the slab. Phase information was extracted in the propagating x-direction at the 15 mm mark where the wave was in the free-space region after passing through the slab. The calculated phase difference was $140 - 80 = 60$ degrees upon switching between the open and closed rings, as shown in Fig. 1(b). The geometrical dimensions of the rings and the numerical setup were the same as the configuration 2 in [29]. Detailed discussion about the numerical methods and parameter extractions can be found in [4, 14, 29]. In the following section we will discuss the experimental setup and the measured data results.

3. EXPERIMENTAL SETUP AND MEASURED DATA

In our free-space experimental measurement setup we utilized two spot-focusing horn lenses as the transmitting and receiving antennas, coaxial cables and a Vector Network Analyzer (VNA) for measuring the transmission/reflection parameters. The spot focusing antennas (model no. 857012X-950/C) manufactured by Alpha Industries, Woburn, Ma (USA), operates in the X-band frequency range. Two equal plano convex lenses were mounted back to back in a conical horn antenna as shown in Fig. 3(a), with one of them responsible for producing an electromagnetic plane wave whilst the other was responsible for focusing it. The $f/\# = f/D$, the ratio of focal length (f) of the lens to antenna diameter (D), is equal to one where D is approximately 30.5 cm. The depth of focus for these horn lens antennas is approximately $10\lambda_0$ and the 3 dB beamwidth is approximately one wavelength. These antennas are effective in terms of minimizing diffraction effect because of its spot focusing feature. Diffraction could be further kept at a minimum by ensuring the sample is three times the E-plane beamwidth which is approximately $3\lambda_0$. Our free-space setup as shown in Fig. 3(a) (without the slab) and the calibration of the transmission and reflection parameters were based on the experimental setup and calibration techniques described in detail in [4, 5]. Such a test up had been very effective for characterizing material properties in free-space.

The transmission/reflection measurements would serve the purpose of locating the resonance and an off-resonance operating frequency for the DSRR slab. The sample was mounted on a 1-D scanner and was aligned with the focus of the lens. The sample consisted of three slabs of FR4 substrate of 1 mm thickness. The middle slab was void of rings and was sandwiched by the top and bottom slabs.
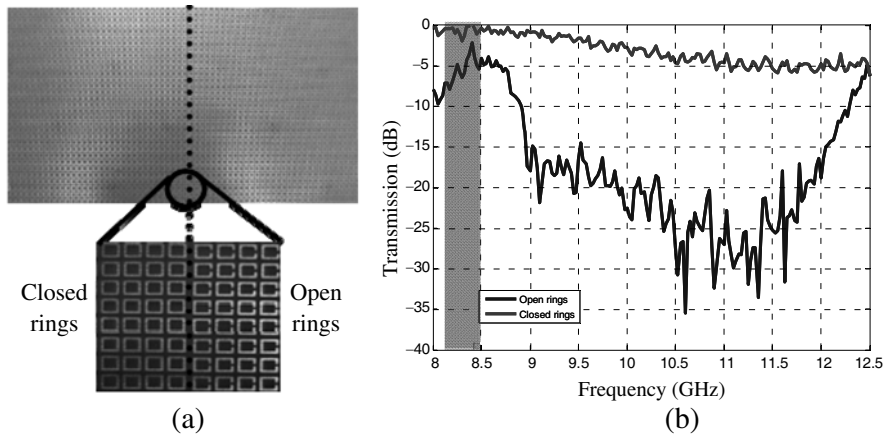
Figure 2. (a) Fabricated structure of the DSRR slab indicating the open and closed rings. (b) Transmission data for the DSRR slab at 8.488 GHz for open and closed rings.

Both sides of the top and bottom slabs were imprinted with copper rings to mimic the DSRRs in the numerical simulation. The ring designs were exposed on the pre-sensitized FR4 substrate using the standard lithography process which were then developed and finally etched by implementing a wet copper etching process. A zoomed-in version of the DSSR slab is shown in Fig. 2(a). The slabs were 300 mm in length and 150 mm in width of which half was composed of closed rings and the other half was occupied by the open rings. The calibration ensured that initially there was zero phase variation and transmission loss in between the spot focusing lenses. The sample was first characterized in terms of transmission for the open rings to locate the resonance of the DSRRs in its open state as shown in Fig. 2(b). This was done by bringing the center of the open rings to the center of the lens and measuring the S_{21} parameters with the VNA connected to the setup through a WR90 coax-to-waveguide connector. Similar measurements were taken for the closed rings as shown in Fig. 2(b). Based on the transmission data we chose to operate at an off-resonant frequency of 8.488 GHz where the transmission loss for both configurations was relatively low [29]. The close proximity of the rings in the double layers of the DSRRs created strong coupling that was responsible for splitting the resonance into two and thereby giving a large bandwidth in the open ring case as noted in Fig. 2(b).
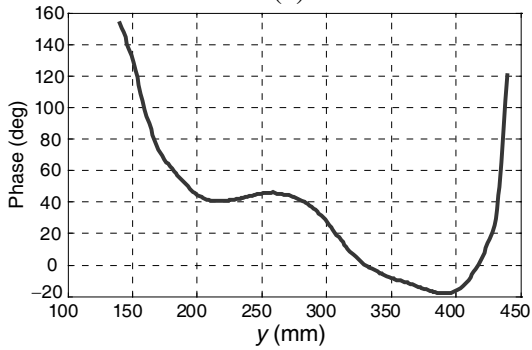
   With the chosen operating frequency, we then opted to measure the phase variation that would occur upon transitioning from closed to
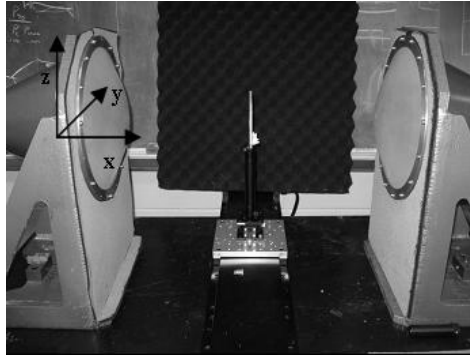
(a)
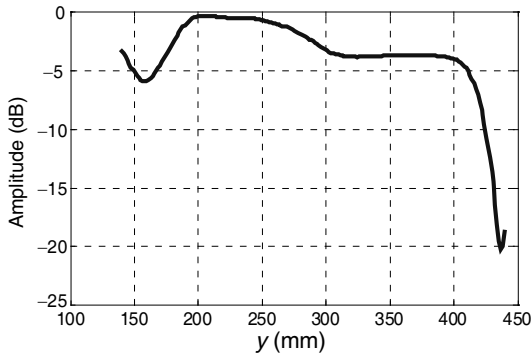
(b)

(c)

Figure 3. (a) 1-D scanning setup consisting of the DSRR slab mounted on an y-axis translational stage and two spot focusing lens horn antennas (b) 1-D scanned data for amplitude variation. (c) 1-D scanned data for phase variation.

open rings. Two sets of experiments were devised in order to calculate the phase change. At first, we performed a 1-D scan of the slab that would effectively record the phase and amplitude variation. The setup for the 1-D scan was similar to the characterization setup with the only distinction of having the sample mounted on a translational stage as shown in Fig. 3(a) along the y-axis. The mounted slab was moved across and in between the two spot focusing antennas by means of our 1-D scanning system. At 8.488 GHz, the distance between the slab and the antenna was one focal length. Within the slab, each section of the closed and open rings was 150 mm×150 mm which was illuminated completely by the spot focusing lens as the 3 dB bandwidth for both E and H field were ($\sim 3\lambda_0 \sim 107$ mm). The E-field was polarized in the z-direction while the slab was scanned in the y axis for 300 mm with a step size of 1.5 mm. Precautions were taken for the unwarranted shaking of the sample as it was translated across by giving few seconds in between each scan so that the sample would stabilize and avoid possible errors. The measured scanned data is shown in Figs. 3(b) and (c) where the phase changes was noted to be 62 degrees. In particular, at the 260 mm mark in the closed ring section the phase was 46 degrees whereas at the 380 mm mark the phase was -16 degrees, producing an overall phase modulation of 62 degrees while transitioning from the closed to the open state of the rings. We also observed a magnitude variation of -2.7 dB for the same transition. Also noted in Figs. 3(b) and (c), measurements at the start and the end mark suffered some edge diffraction effects as the slab was only partially illuminated by the focused beam.

We further verified the phase variation phenomenon using metamaterials with a 2-D measurement scheme at the same operating frequency of 8.488 GHz, analogous to the previous 1-D experiments. For this measurement setup, the receiving antenna was replaced by a probe polarized in the direction of the electric field parallel to the z-axis. On the transmitting end, one of the plano convex lenses was removed so that only plane wave was produced to illuminate the structure. The probe was 25 mm away from the slab mounted on a y-z scanner and offset by a rexolite rod to minimize the scattering from the scanning parts. A Teflon enclosure with an opening in the middle was used to mount the sample. The edges of the Teflon enclosure were fenced with metal to mimic a peep-hole. The setup is shown in Fig. 4. At first, we scanned the opening area without the sample loaded and measured the phase variation within that area. We noted that both the amplitude and phase variation was negligible ensuring that we have plane wave within that region illuminated by the transmitting antenna. This is shown in Figs. 5(a) and (b), where a region of 40 mm (1.1λ)

in the z-direction and 130 mm (3.7λ) in the y-direction was scanned
with a 1.5 mm step size. Following that, the sample was mounted
and scanned for the same area to measure the phase variation while
transitioning from closed to open rings. Thus for the given scanned
region, the area constituted of 26 rings with 13 rings in the y direction
and 10 rings in the z direction of each kind respectively. The 2-D
measured result of the metamaterial-loaded slab and normalized to the
free-space measurement is shown in Figs. 5(c) and (d). The transition
point between the open and closed rings was 405 mm mark. We noted
from the spatial data that the amplitude varied by 1.2 dB while the
phase changed by 74 degrees at an half-wavelength distance on either
side of the transition point and upon averaging the z-axis data. The
2-D scanned data served as a good proof-of-concept for phase variation
on switching from open to closed state of the rings.

4. DISCUSSION OF THE MEASURED DATA

The numerical results obtained from simulation suggested that a phase
variation with minimal loss can be obtained using a stack of tunable
DSRRs when excited by the electric field polarized along the gap of
the rings for a particular frequency range. We noted there was a slight
shift in the operating frequency ($\sim$2%) in the experiments from the
numerical one, which can be accounted for the fabrication errors in
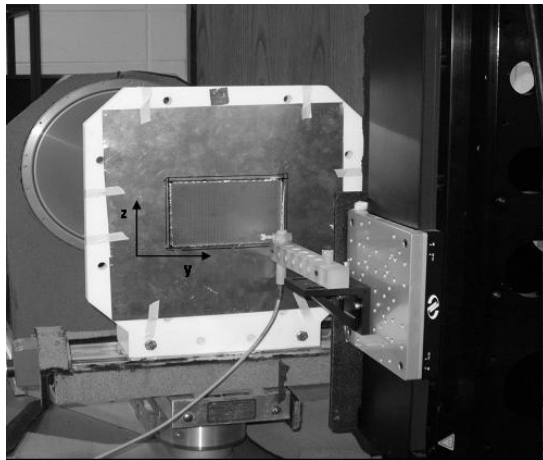the rings and the material properties of host dielectrics. The loss

Figure 4. 2-D scanning setup consisting of a scanning probe mounted
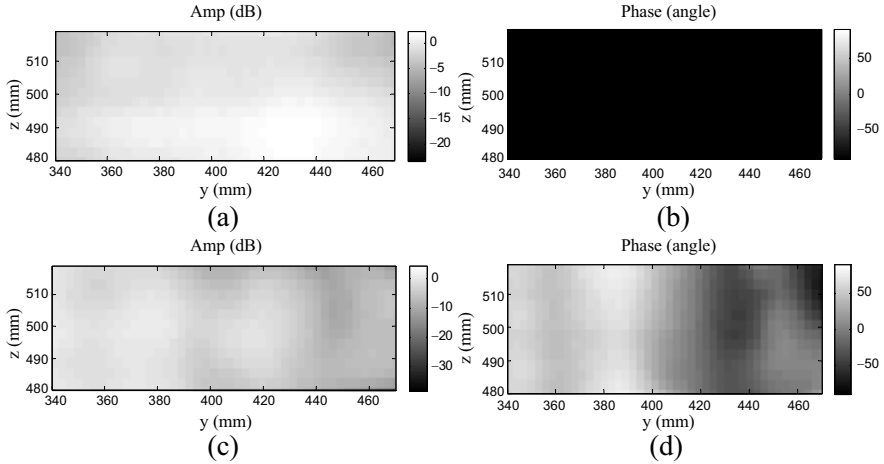on a y-z stage and a lens horn antenna as the source.

Figure 5. (a) and (b) Two dimensional scanned data of amplitude and phase variation in free space respectively. (c) and (d) Two dimensional scanned data of amplitude and phase variation of the DSRR slab respectively.

was considerably higher using the FR4 substrate compared to our previous study [29] where we used Duroid substrate. In particular, in our simulation results, while switching between the closed and open rings, we noted a 0.8 dB amplitude variation with Duroid substrate and 1 dB variation with the FR4 substrate. This can be understood in terms of the dielectric constants, where higher transmission loss and impedance mismatch might have occurred due to FR4 substrate's higher permittivity value ($\varepsilon = 4.4$) compared to Duroid's ($\varepsilon = 2.2$). Nevertheless, the measured data served the purpose of proof-of-concept and improved results can be obtained with low loss material. In this paper, the measured data matched well with the numerical results. Particularly, we observed that the phase variation in our numerical and theoretical results was 60 degrees whereas according to the 1-D scanned data the phase change was 62 degrees. With our 2-D scanned data the phase modulation was 74 degrees. The slight variation in the result may have been due to the diffraction effect in our 2-D setup where a monopole was used to scan the received signal from a plane wave illuminating the structure compared to our 1-D scanning system that had spot-focusing lens to transmit and receive signal minimizing diffraction effects. Our demonstration of phase modulation in the RF frequency is still for a narrowband frequency range which we plan to overcome in the future by employing broadband materials such as in [24]. To date, switching between the two states of the DSRRs is

static. We plan to employ electrical techniques to make the switching process dynamic [26].

5. CONCLUSION

In this paper, we experimentally demonstrated phase modulation in the X-band frequency range using metamaterials such as the planar slabs of DSRRs by exciting the structure with the electric field polarized along the gap of the rings. Numerical simulations of the DSRRs showed a phase modulation of 60 degrees could be obtained on switching between the open and closed state of the DSRRs. Two sets of experiments were performed in the free-space to scan the metamaterial slab in both one and two dimensions. The measured data matched well with the simulated data. The results presented here are encouraging for practical applications such as phased array antennas, beam forming and beam scanning systems. In our future work, we plan to demonstrate broadband dynamic phase modulation with metamaterials.

REFERENCES

1. Veselago, V. G., "The electrodynamics of substances with simultaneously negative values of permittivity and permeability," *Sov. Phys. Uspekhi*, Vol. 10, 509–514, 1968.
2. Shelby, R. A., D. R. Smith, and S. Schultz, "Experimental verification of negative index of refraction," *Science*, Vol. 292, 77–79, 2001.
3. Lu, Z., J. A. Murakowski, C. A. Schuetz, S. Shi, G. J. Schneider, and D. W. Prather, "Three-dimensional subwavelength imaging by a photonic-crystal flat lens using negative refraction at microwave frequencies," *Phys. Rev. Lett.*, Vol. 95, 153901(4), 2005.
4. Sheng, Z. and V. Varadan, "Tuning the effective properties of metamaterials by changing the susbstrate," *J. Appl. Phys.*, Vol. 101, 014909-1, 2007.
5. Ghodgaonkar, D. K., V. V. Varadan, and V. K. Varadan, "Free-space measurement of complex permittivity and complex permeability of magnetic materials at microwave frequencies," *IEEE Trans. Instrum. Meas.*, Vol. 39, 387–394, 1990.
6. Aydin, K., I. Bulu, K. Guven, M. Kafesaki, C. M. Soukoulis, and E. Ozbay, "Investigation of magnetic resonances for different split-ring resonator parameters and designs," *New J. Phys.*, Vol. 7, 168, 2005.

7. Aydin, K., K. Guven, N. Katsarakis, C. M. Soukoulis, and E. Ozbay, "Effect of disorder on magnetic resonance band gap of split-ring resonator structures," *Opt. Express*, Vol. 12, 5896, 2004.

8. Zharov, A. A., I. V. Shadrivov, and Y. S. Kivshar, "Nonlinear properties of left handed materials," *Phys. Rev. Lett.*, Vol. 91, 037401, 2003.

9. Chen, H. T., W. J. Padilla, J. Zide, A. Gossard, A. Taylor, and R. Averitt, "Active terahertz metamaterial devices," *Nature*, Vol. 444, 597–600, 2006.

10. Logeeswaran, V. J., A. Stameroff, M. Islam, W. Wu, A. Bratkovsky, P. Kuekes, S. Wang, and R. Williams, "Switching between positive and negative permeability by photoconductive coupling for modulation of electromagnetic radiation," *Appl. Phys. A*, Vol. 87, 209–216, 2007.

11. Reynet, O. and O. Acher, "Voltage controlled metamaterial," *Appl. Phys. Lett.*, Vol. 84, 1198, 2004.

12. He, P., P. Parimi, and C. Vittoria, "Tunable negative refractive index metamaterial phase shifter," *Elec. Lett.*, Vol. 43, 2007.

13. Velez, A. and J. Bonache, "Varactor-loaded complementary split ring resonators VLCSRR and their application to tunable metamaterial transmission lines," *IEEE Microwave and Wirel. Compon. Lett.*, Vol. 18, 28–30, 2008.

14. Smith, D., S. Schultz, P. Markos, and C. M. Soukoulis "Determination of effective permittivity and permeability of metamaterials from reflection and transmission coefficients," *Phys. Rev. B*, Vol. 65, 195104-1, 2002.

15. Chen, H.-T., J. Ohara, A. Azad, A. Taylor, R. Averitt, D. Shrekenhamer, and W. J. Padilla, "Experimental demonstration of frequency-agile terahertz metamaterials," *Nature Photonics*, Vol. 2, 295–298, 2008.

16. Karkkainen, M. K. and P. Ikonen, "Patch antenna with stacked split-ring resonators as artificial magneto-dielectric substrate," *Microwave Opt. Technol. Lett.*, Vol. 46, 554–556, 2005.

17. Oh, S. and L. Shafai, "Artificial magnetic conductor using split ring resonators and its applications to antennas," *Microwave Opt. Technol. Lett.*, Vol. 48, 329–334, 2006.

18. Maslovski, S., P. Ikonen, I. kolmakov, and S. Tretyakov, "Artificial magnetic materials based on the new magnetic particle: Metalsolenoid," *Progress In Electromagnetics Research*, PIER 54, 61–81, 2005.

19. Katsarakis, N., T. Koschny, and M. Kafesaki, "Electric coupling to the magnetic resonance of split ring resonators," *Appl. Phys. Lett.*, Vol. 84, 2943–2945, 2004.

20. Pendry, J. B., D. Schurig, and D. R. Smith, "Controlling electromagnetic fields," *Science*, Vol. 312, 1780–1782, 2006.

21. Kafesaki, M., T. Koschny, R. Penciu, T. Gundogdu, E. Econonou, and C. Soukoulis, "Left-handed metamaterials: Detailed numerical studies of the transmission properties," *J. Opt. A: Pure and Appl. Opt.*, Vol. 7, S12–S22, 2005.

22. Dudley, D., W. Duncan, and J. Slaughter, "Emerging digital micromirror device DMD applications," *Proc. SPIE*, Vol. 4985, 14–25, 2003.

23. Aydin, K. and E. Ozbay, "Capacitor-loaded split ring resonators as tunable metamaterial components," *J. Appl. Phys.*, Vol. 101, 024911-5, 2007.

24. Liu, N., H. Guo, L. Fu, S. Kaiser, H. Schweizer, and H. Giessen, "Three-dimensional photonic metamaterials at optical frequencies," *Nature Materials*, Vol. 7, 31–37, 2008.

25. Balanis, C., *Antenna Theory*, Chap. 6, 3rd edition, John Wiley & Sons, 2005.

26. Hand, T. and S. Cummer, "Controllable magnetic metamaterial using digitally addressable split-ring resonator," *IEEE Ant. Propag. Lett.*, to be published.

27. Lim, S., C. Caloz, and T. Itoh, "Metamaterial-based electronically controlled transmission-line structure as a novel leaky-wave antenna with tunable radiation angle and beamwidth," *IEEE Trans. Micro. Theo. Tech.*, Vol. 53, 161–173, 2005.

28. Chen, H.-T., W. J. Padilla, M. J. Cich, A. K. Azad, R. D. Averitt, and A. J. Taylor, "A metamaterial solid state terahertz phase modulator," *Nature Photonics*, Vol. 3, 148–151, 2009.

29. Mirza, I. O., S. Shi, and D. W. Prather, "Phase modulation using dual split ring resonators," *Opt. Express*, Vol. 17, 5089–5097, 2009.